Heliyon 9 (2023) e13290

Contents lists available at ScienceDirect

Heliyon

journal homepage: www.cell.com/heliyon

Research article

Liquiritin inhibits MRGPRX2-mediated pseudo-allergy through the PI3K/AKT and PLCγ signaling pathways

Lu Wang [a,*], Chuyue Huang [a], Zhili Li [a], Guizhou Hu [b], Jin Qi [b], Zhimin Fan [a,**]

[a] Nanjing Hospital of Chinese Medicine Affiliated to Nanjing University of Chinese Medicine, Nanjing, 210022, PR China
[b] China Pharmaceutical University, Nanjing, 211198, PR China

ARTICLE INFO

Keywords:
Liquiritin
Anti-Pseudo-allergy
MAS-Related G protein-coupled receptor-X2
PI3K/AKT
PLCγ
Immunopharmacology

ABSTRACT

Liquiritin is a natural flavone with a variety of pharmacological effects derived from the medicinal food homology plant *Glycyrrhiza uralensis Fisc*h. As a kind of lethal allergic reactions, pseudo-allergic reactions (PARs) arise from the Mas-related G protein coupled receptor X2 (MRGPRX2)-triggered fast degranulation of mast cells (MCs). In the current work, the anti-pseudo-allergy action and potential mechanisms of liquiritin were explored *in vivo* and *in vitro*. Liquiritin suppressed the calcium influx and degranulation elicited by Compound 48/80 (C48/80) in mouse peritoneal mast cells (MPMCs). In mice, liquiritin also inhibited the C48/80-elicited hind paw extravasation, as well as the elevations in TNF-α and histamine levels. Molecular docking combined with detection of HEK293T cells expressing human MRGPRX2 showed that liquiritin was a potential MRGPRX2 antagonist and inhibited PARs through the PI3K/AKT and PLCγ signaling pathways downstream of MRGPRX2. The present work opens a new avenue for the PARs management.

1. Introduction

As a lethal allergic reaction, anaphylaxis arises from the fast degranulation of mast cells (MCs) through the high-affinity IgE receptor (FcεRI) accumulation. Reacting to the US FDA-approved drugs, however, MCs also degranulate to incur pseudo-allergic reactions (PARs) [1]. Common mediators of PARs, including neuromuscular blockers, opioids and fluoroquinolone antibiotics (e.g. ciprofloxacin), enable the Mas-related G protein coupled receptor X2 (MRGPRX2)-induced initiation of human MCs and the elicitation of secretion of histamine and other vascular-inflammatory substances. They always occur quickly and cause redness, itching, rash or breathing difficulties resembling those of generalized anaphylaxis [2]. Current treatments for allergic-like diseases are primarily MC stabilizers, antihistamines and immune suppressors, which merely allow mitigation of anaphylaxis-induced suffering and are conducive to easing allergic symptoms. The above drugs, however, have a few adverse effects [3]. Therefore, special natural ingredients with low toxicity for PARs are scarce and still to be investigated further.

Liquiritin, as a primary flavone derivative of medicinal plant *Glycyrrhiza uralensis Fisc*h, also known as licorice (Gan-Cao in Chinese) [4], is applied extensively for Traditional Chinese Medicine (TCM) or food additive purpose [5]. Its diverse pharmacological traits have been confirmed, including anti-inflammatory [6], anti-nociceptive [7], neuroprotection [8], antioxidant and cardioprotective effects [9,10]. Our previous study suggested that licorice extract could suppress the calcium influx and MC degranulation elicited by C48/80,

* Corresponding author.
** Corresponding author.
E-mail addresses: wanglu@njucm.edu.cn (L. Wang), fanzm@njucm.edu.cn (Z. Fan).

https://doi.org/10.1016/j.heliyon.2023.e13290
Received 14 November 2022; Received in revised form 22 December 2022; Accepted 26 January 2023
Available online 31 January 2023

but whether it is related to liquiritin remains unclear.

The present study assessed the anti-pseudo-allergic action of liquiritin in the *in-vitro* mouse peritoneal mast cells (MPMCs) and the *in-vivo* mice. The liquiritin–MRGPRX2 interplay was identified via molecular docking and the calcium response in MRGPRX2-HEK293T cells. Finally, the mechanism whereby liquiritin resists the pseudo-allergy was explored.

2. Materials and methods

2.1. Drugs and reagents

Fetal bovine serum (FBS) used was the Gibco (Grand Island, NY) product. Compound 48/80 (C48/80), poly-D-lysine hydrobromide (PDL) and *p*-nitrophenyl-N-acetyl-β-D-glucosaminide were the Sigma Aldrich (Saint Louis, MO) products. Triton X-100 was procured from Amresco (Solon, OH). Liquiritin was procured from Yuanye Biotechnology (Shanghai, China). Penicillin, streptomycin, Fluo-4 AM and RIPA lysis buffer were obtained from Beyotime Biotechnology (Shanghai, China). TNF-α and histamine ELISA kits were procured from Meimian Industrial (Yancheng, China). A plasmid with MRGPRX2 was constructed by GENERAL BIOL (Anhui, China). Anti-TNF-α antibody (ab205587) was the product of Abcam (Cambridge, England). Lipofectamine 2000 and Opti-MEM were the Invitrogen (Carlsbad, CA) products. Monoclonal GAPDH antibody (60004-1-Ig), HRP-conjugated Affinipure Goat Anti-Mouse IgG (H + L) (SA00001-1) and Anti-Rabbit IgG (H + L) (SA00001-2) were procured from Proteintech (Wuhan, China).

2.2. Animals and ethical statement

Male ICR mice weighing 18–22 g, which were procured from Yangzhou University (Yangzhou, China), were housed at 22 °C and 55 ± 5% RH with a 12-h light:12-h dark photocycle, and fed and watered ad libitum. All animal experiments were performed according to the Guide for the Care and Use of Laboratory Animals and complied with ARRIVE guidelines in a licensed laboratory for animal experiments (license number: SYXK (Su) 2018–0049). The study was reviewed and approved by the Laboratory Animal Ethics Committee of Nanjing University of Chinese Medicine on the management and use of laboratory animals.

2.3. Cell lines and cell culture

Through transient transfection, we constructed the HEK293T cells expressing human MRGPRX2 (MRGPRX2-HEK293T cells) and negative controls (NC-HEK293T cells). After seeding onto a 24-well microplate, the HEK-293T cells were kept overnight. Opti-MEM medium was utilized to dilute the plasmid (Cloning vector: pcDNA3.1 (+)) and transfection reagent, which were then mixed at a ratio of 1 μg: 2.5 μL for 20 min. Then, the DNA-lipid complex was added to every well for 6 h. Finally, cultivation of MRGPRX2-HEK293T and NC-HEK293T cells was accomplished in complete medium under 37 °C and 5% CO_2 conditions. Quantitative real-Time polymerase chain reaction (qRT-PCR) was applied with the purpose of assessing the transfection and expression efficiencies.

2.4. Isolation of MPMCs

After sacrificing adult male mice, 2 sequential peritoneal lavages were carried out with 10 mL of ice-cold phosphate-buffered saline (PBS) in total, which were then combined and subjected to a 10-min centrifugation under 800×*g* and 4 °C conditions. Next, the supernatant was discarded and the small residual mast cell pellet (~2 mL) was added sequentially with 30% and 80% Percoll (2 mL) to form an interface (final volume proportion: 1:1:1). Following a 15-min centrifugation under 600×*g* and 4 °C conditions, the cells at the junction interface were gathered and subjected to twice washing in PBS (200 *g*, 4 °C) for 10 min. Finally, a 10% FBS-involving DMEM was utilized to resuspend the MPMCs, and then their purity was assayed by staining with toluidine blue, while their viability was assayed by trypan blue exclusion.

2.5. Cytotoxicity assay

Cellular toxicity was assayed by the MTT method. Each 3×10^4 MPMCs were inoculated per well of a 96-well microplate. Based on incubation for 12 h at 37 °C with 5% CO_2, varying concentrations of test compounds were utilized to treat the MPMCs for 60 min. The supernatant was then discarded, and the MPMCs were incubated in MTT (0.5 mg/mL)-involving DMEM under 37 °C and 5% CO_2 conditions. Four h later, the medium was removed and each well was supplemented with dimethyl sulfoxide to 150 μL. Finally, 570- and 650-nm values of absorbance were determined.

2.6. β-Hexosaminidase release assay

After 24 h of cultivation in a 96-well microplate at 3×10^4 cells per well, the MPMCs were washed using FBS-free DMEM, and then subjected to a 30-min incubation in DMEM involving varying concentrations of liquiritin at 37 °C with 5% CO_2. Meanwhile, DMEM alone was utilized to treat the blank control and model (C48/80) group cells. Then, a 30-min proceeded on the cells in liquiritin groups and model group using C48/80 (30 μg/mL) under 37 °C and 5% CO_2 conditions. FBS-free DMEM was utilized for incubating the blank control cells.

β-Hexosaminidase assays were run exactly as previously described [11]. For the quantification of β-hexosaminidase released into

the cellular lysate and supernatant, the *p*-nitrophenyl-N-acetyl-β-D-glucosamide was hydrolyzed for 60 min in 0.1 M pH-4.5 sodium citrate buffer at 37 °C. Determination of 405-nm absorbance proceeded for every well. The computational equation for the β-hexosaminidase release ratio was as shown below:

$$\beta - \text{hexosaminidase}(\%) = \frac{\text{OD(supernatant)}}{\text{OD(supernatant)} + \text{OD(lysate)}} \times 100$$

2.7. Intracellular Ca^{2+} Concentration ($[Ca^{2+}]_i$) assay

The Fluo-4 AM fluorescence indicator was used for the $[Ca^{2+}]_i$ determination. After seeding onto a 96-well microplate involving 50 μg/mL PDL, the MPMCs were equilibrated for 24 h under 37 °C and 5% CO_2 conditions, and then treated for 30 min with varying sample solutions, followed by a 40-min loading with Fluo-4 AM under 37 °C and 5% CO_2 conditions. Next, a pH 7.4 Locke's buffer involving HEPES (2.144 g/L), glucose (1.009 g/L), sodium chloride (9 g/L), potassium chloride (0.417 g/L), calcium chloride (0.256 g/L), magnesium chloride (0.096 g/L) and 500 μL of glycine (0.1 mM) was used to wash the MPMCs 4 times, and the final volume per well was made to 150 μL. Subsequently, the microplate was shifted to a Varioskan Multifunctional microplate reader 3001 (Thermo Fisher Scientific, Germany). Cellular excition wavelength was determined at 488 nm, while the emission detection wavelength was 520 nm. For the baseline establishment, continuous fluorescence scanning was carried out for 25 s. Afterwards, varying sample wells and model (C48/80) wells were added with 50 μL of C48/80 (120 μg/mL, 4 ×) to make the final volume per well 200 μL. The control wells were added with Locke's buffer. Finally, 125 s of continuous fluorescence scanning was carried out.

After seeding onto a 6-well microplate involving PDL (50 μg/mL), the NC-HEK293T or MRGPRX2-HEK293T cells were equilibrated for 24 h under 37 °C and 5% CO_2 conditions, and then treated for 30 min with varying concentrations of liquiritin solutions. Varying sample wells and model (C48/80) wells were supplemented with C48/80 (150 μg/mL, 3 ×) to 500 μL. After 10 min, the cells were subjected sequentially to a 30-min incubation using Fluo-4 AM (final concentration: 1 μM) in PBS at 37 °C, thrice washing in PBS and an extra 15-min incubation without Fluo-4 AM to accomplish the dye de-esterification. Final step was the assessment of fluorescence intensity under excitation and emission wavelengths of 494 and 516 nm with flow cytometry (BECKMAN COULTER CytoFLEX).

2.8. Hind paw swelling

Mice were randomized into 4 groups (n = 8), with 3 treatment groups (intraperitoneally injected with liquiritin at 1, 2 and 4 mg/kg), and 1 blank control group (injected with saline). Thirty minutes later, the mice were anesthetized by 1% intraperitoneal phenobarbital administration (0.2 mL), and 15 min later, every mouse was administered 0.4% Evans blue in saline (0.2 mL) intravenously. The blank control was given 5 μL of saline at the left paw. Right paw injection of 30 μg/mL C48/80 in saline proceeded after 5 min. Finally, paw thickness was re-measured 15 min later, and documented.

2.9. Histological analysis

Murine grouping and treatment procedures were identical to those in Section *2.8*. Fifteen minutes after right paw injection of 30 μg/mL C48/80, the paw skin at the injection site was excised, PBS-washed and immobilized in 4% formaldehyde for 48 h, followed by staining with H&E and toludine blue. Immediately afterwards, an OLYMPUS X73-A21PH microscope (Tokyo, Japan) was utilized for image capturing.

2.10. Histamine and TNF-α release assay

Mice were randomized into 5 groups (n = 8), with 3 treatment groups, 1 blank control group and 1 model (C48/80) group. The treatment groups were administered oral liquiritin at varying doses, while the blank control and model (C48/80) groups were given saline. Thirty min later, the treatment and model groups were challenged by injecting 2.5 mg/kg C48/80 intravenously, while intravenous saline was given to the blank control group. Blood was sampled 10 min later, and serum was acquired via a 10-min centrifugation (825 *g*, ambient temperature). Serum histamine and TNF-α were assayed as per the protocols of ELISA histamine kits.

We randomized the mice into 4 groups (n = 8), comprising 3 treatment groups and 1 blank control group. After completing the experimental steps described in *2.8*, the murine hind paw skin tissues were harvested, washed in PBS twice, added with RIPA lysis solution involving phosphatase inhibitor (2%) and PMSF (1%), and then pulverized in a grinder. Collection of supernatant proceeded through a 10-min centrifugation (10,000 r/min, 4 °C) for the Western blot assessment of TNF-α.

2.11. Western blot analysis

After 24 h of cultivation in a 6-well microplate at 5×10^5 cells per well, the MPMCs were washed using FBS-free DMEM, and then subjected to a 30-min incubation in DMEM involving varying concentrations of liquiritin at 37 °C with 5% CO_2. Meanwhile, DMEM alone was utilized to treat the blank control and model (C48/80) groups. Then, a 30-min proceeded on the cells in liquiritin groups and model group using C48/80 (30 μg/mL) under 37 °C and 5% CO_2 conditions. FBS-free DMEM was utilized for incubating the blank control cells.

After sampling of cells or tissues, a RIPA lysis buffer was utilized to lyse cells, followed by the protein level quantification with a

BCA protein assay kit. Equivalent amounts of protein from the total cellular lysates (30 μg/lane) were isolated by10% SDS–PAGE gels (BioRad Laboratories, CA), shifted onto the NC membranes (BioRad Laboratories, CA) by wet transfer, blotted using specific primary antibodies (PI3K [1:1000], p-PI3K [1:1000], Akt [1:1000], *p*-Akt [1:1000], PLCγ [1:1000], *p*-PLCγ [1:1000] and TNF-α [1:1000] antibodies) and subsequently probed with isotype-specific horseradish peroxidase-tagged secondary antibodies. A CLINX + system (CLINX, China) was exploited to examine the bound immunocomplexes.

2.12. qRT-PCR analysis

Following extraction of total RNA from cells by adoptingTRIzol reagent (1 mL; Invitrogen, USA), 1 μg of the total RNA extract was transcribed reversely as per the protocol of Superscript II reverse transcriptase (Yeasen, Shanghai, China) using oligo (T) primers. SYBR Green PCR Master Mix (Yeasen, Shanghai, China) was utilized to quantify the expression of gene on an ABI7300. Next step was normalization of gene expression levels in every cDNA sample to those of internal GAPDH. For every date point, the experiments were triplicated. The following primer pairs were adopted for PCR. MRGPRX2-F: CTGGTAGGAAACGGGTTTGTG, MRGPRX2-R: GCTGAGGACGTAGACAGAGAAG, GAPDH-F: CTGGGCTACACTGAGCACC, GAPDH-R: AAGTGGTCGTTGAGGGCAATG.

2.13. Molecular docking

With the purpose of exploring the ligands–receptors interactions, the Glide Mode of Maestro interface (Schrödinger Suite, LLC, NY) was used to accomplish the molecular docking. The source of MRGPRX2 docking model adopted herein was the Research Collaboratory for Structural Bioinformatics Protein Data Bank (RCSB PDB) [12].

2.14. Statistical analysis

The entire analyses were carried out with the aid of Prism v5.01 (GraphPad Software, La Jolla, CA). Data were statistically processed via analysis of variance (ANOVA) and expressed as means ± SEMs. Pairwise comparisons were made through two-tailed tests, while multiple comparisons were done through one-way ANOVA and subsequent Dunnett's test. The *p*-values of<0.05 were regarded as to be of statistical significance (*$p < 0.05$, **$p < 0.01$, and ***$p < 0.001$). Every experiment was at least triplicated.

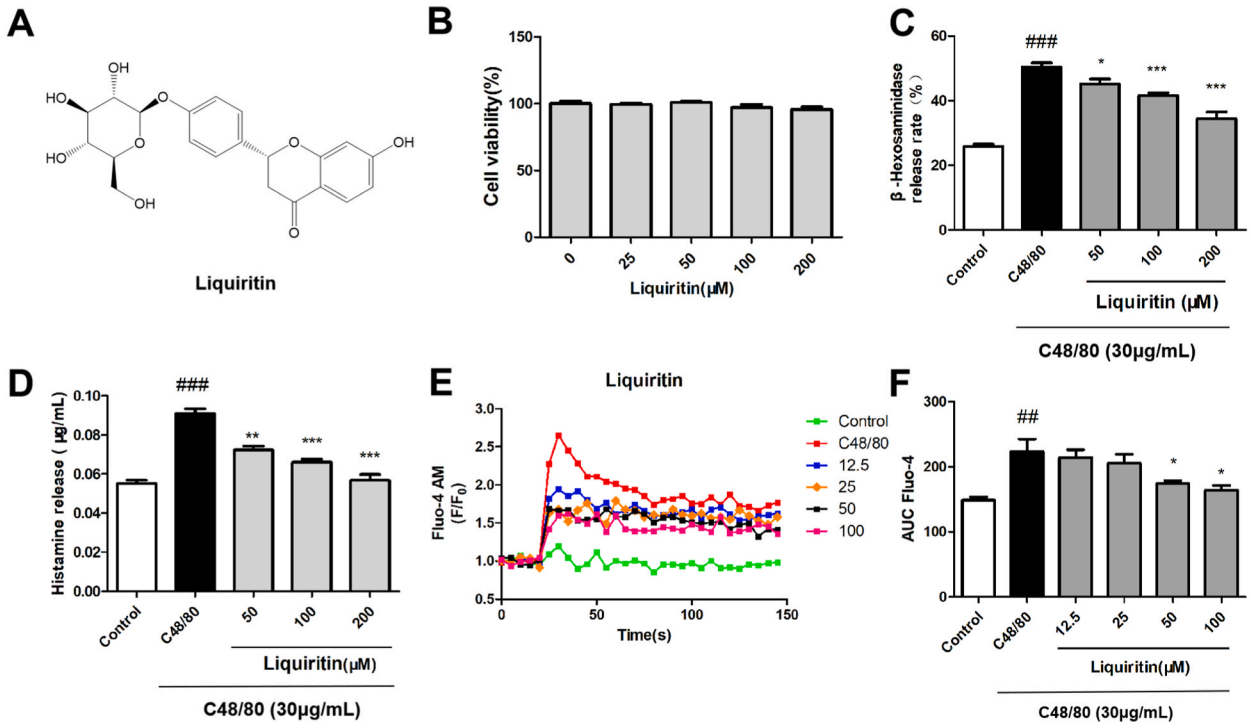

Fig. 1. In MPMCs, the C48/80-triggered degranulation and calcium influx were suppressed by liquiritin. (A) Chemical structure of liquiritin. (B) Toxicity of liquiritin on MPMCs. Liquiritin showed negligible cytotoxicity to MPMCs below 200 μM. (C) Liquiritin suppressed the β-hexosaminidase discharge elicited by C48/80 in MPMCs. (D) Liquiritin suppressed the histamine discharge elicited by C48/80 in MPMCs. (E) Liquiritin dose-dependently reduced the calcium influx elicited by C48/80. (F) Quantitative outcome of doseeresponse correlation for liquiritin. Data expressed are means ± SEMs. $^{###}p < 0.001$, 30 μg/mL C48/80 group vs. control group. $^{*}p < 0.05$, $^{**}p < 0.01$, $^{***}p < 0.001$, vs. C48/80 group.

3. Result

3.1. Liquiritin inhibited C48/80-induced degranulation and calcium influx in MPMCs

As shown in Fig. 1A, liquiritin is a flavonoid in licorice. First, its role in the MPMC viability was assayed by the MTT method. Liquiritin presented minimal cytotoxicity against MPMCs at a concentration of 200 μM (Fig. 1B). Upon MC activation, the preformed inflammatory mediators like β-hexosaminidase, synthetic cytokines and histamine were secreted quickly. To assess liquiritin's role in C48/80-induced MC degranulation, we quantified the β-hexosaminidase and histamine releases. The discharge of both β-hexosaminidase (Fig. 1C) and histamine (Fig. 1D) from MPMCs was inhibited prominently by liquiritin. In PARs, the elevation of intracellular Ca^{2+} levels is the primary determinant for the degranulation of MCs [13]. Hence, we explored how liquiritin influenced the Ca^{2+} mobilization in MPMCs. The C48/80-triggered calcium influx decreased following liquiritin pretreatment in a dose-dependent fashion (Figs. 1E and F). This implies that through the calcium signaling pathway, liquiritin reduced the degranulation elicited by C48/80.

3.2. Liquiritin suppressed C48/80-induced local inflammation

After confirming the *in-vitro* inhibitory action of liquiritin against MC activation, we next assessed its effects on C48/80-induced paw edema in mice. Intragastric liquiritin administration was given to the treatment group at varying concentrations, and 30 min later, the murine right hind paws were injected with 30 μg/mL C48/80 in saline (5 μL). Meanwhile, the left hind paws were administered an equivalent volume of saline to serve as a control. It is clear from Figs. 2A and B that following the liquiritin injection, the hind paw thickness declined with the liquiritin dose. As revealed by the H&E staining of paw skin, liquiritin suppressed the histamine-triggered vasodilatation (Fig. 2C). Meanwhile, the results of toluidine blue staining demonstrated that the degranulated MC counts dropped drastically following injection of liquiritin (Fig. 2D).

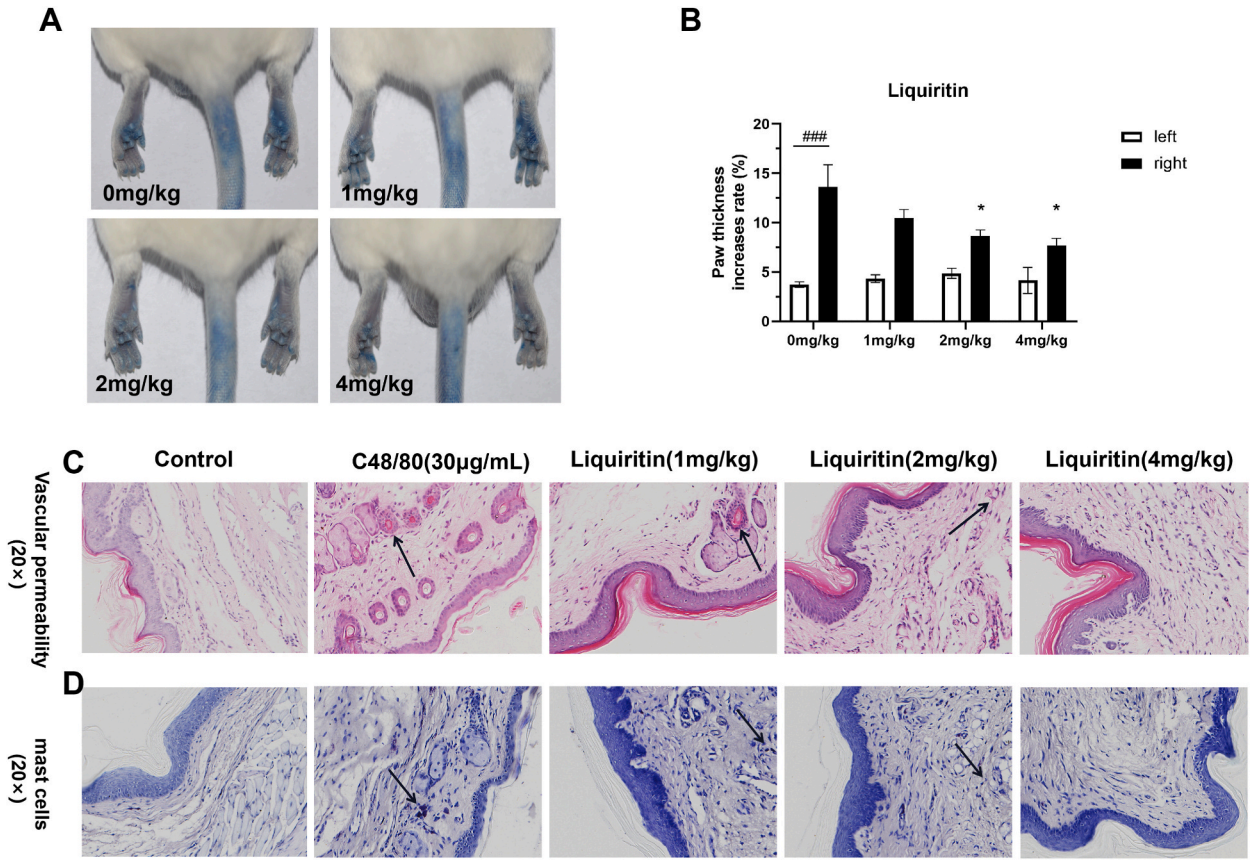

Fig. 2. Liquiritin suppressed C48/80-induced local inflammation. (A,B) Liquiritin decreased the degree of swelling induced by C48/80 in the hind paws of mice. (C) H&E staining of mice hind paw skin. Liquiritin inhibited vascular exudation in a dose-dependent manner. (D) Murine hind paw skin stained with Toluidine blue. Liquiritin suppressed the MC degranualtion elicited by C48/80. Data expressed are means ± SEMs. $^{###}p < 0.001$, right against left paw comparisons in blank control group. $^{*}p < 0.05$, right paw comparisons between treatment and blank control groups.

3.3. Liquiritin reduced the release of histamine and TNF-α in mouse serum and skin tissue

For further verification of liquiritin's anti-pseudo-allergic action *in vivo*, after 30 min of intragastric administration of different doses of liquiritin, systemic anaphylaxis was induced by the tail venous administration of C48/80 (2.5 mg/kg).From every group, murine blood was sampled and then centrifuged, followed by assaying of the serum histamine and TNF-αreleases by ELISA kits. The results showed that liquiritin attenuated the C48/80-elicitedexpressionelevations of histamine (Fig. 3A) and TNF-α (Fig. 3B) evidently. Moreover, the tissue level of TNF-α in the murine paw skin (Fig. 3C) was also inhibited significantly. The foregoing results collectively proved that the liquiritin can resist pseudo-allergies *in vivo*.

3.4. Liquiritin is a potential ligand of MRGPRX2

Molecular docking assays revealed that liquiritin was capable of binding to the MRGPRX2 receptor with high matching degree

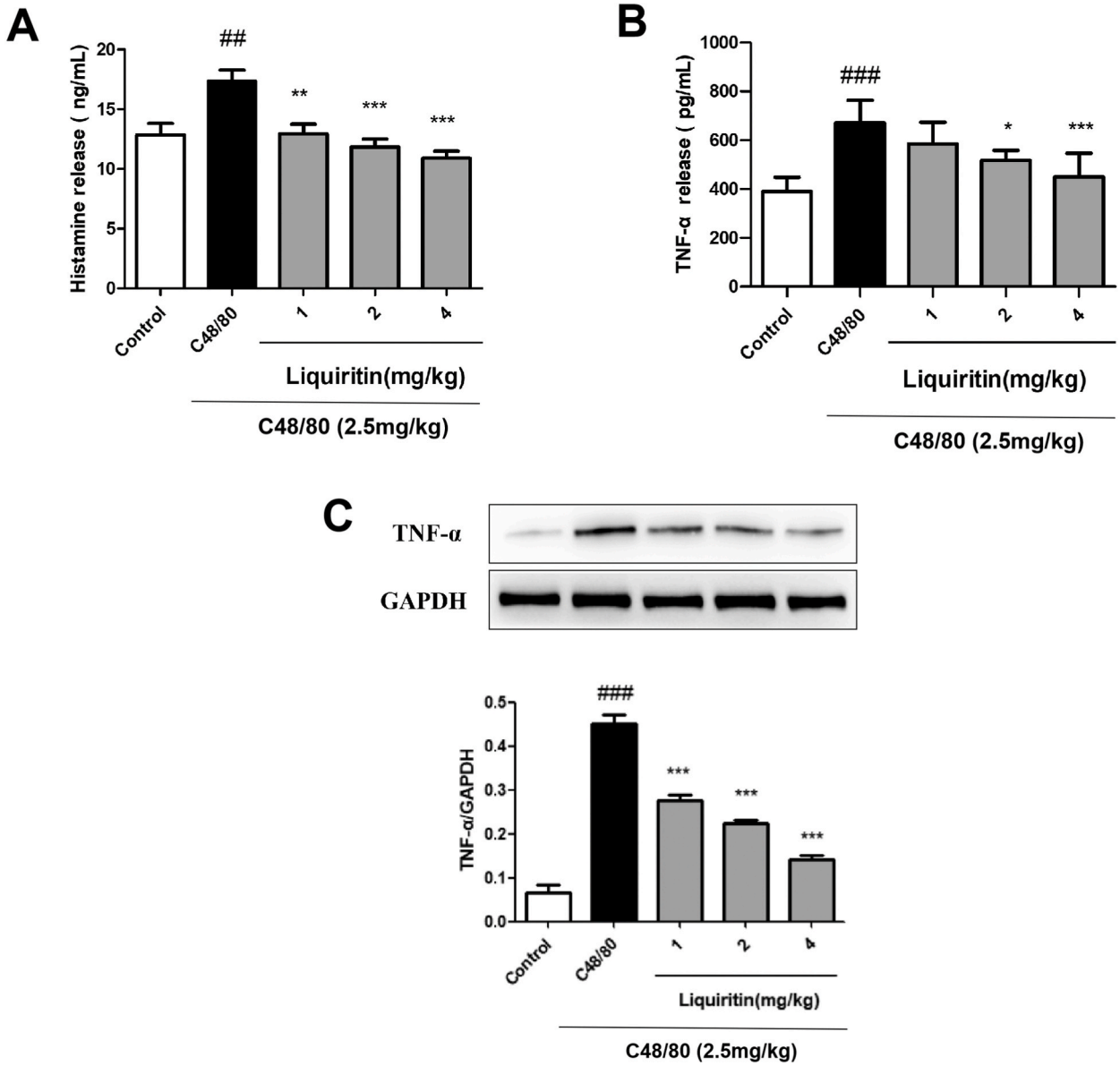

Fig. 3. Liquiritin suppressed the MC degranualtion elicited by C48/80 in mice. (A) Liquiritin inhibited C48/80-induced increase of histamine in mice serum. (B) Liquiritin inhibited C48/80-induced TNF-α in mice serum. (C) Liquiritin inhibited increase of TNF-α in mice skin tissue sections. Data expressed are means ± SEMs. $^{\#\#}p < 0.01$, $^{\#\#\#}p < 0.001$, C48/80 group vs. control group. $^{*}p < 0.05$, $^{**}p < 0.01$, $^{***}p < 0.001$, treatment groups vs. C48/80 group.

(Fig. 4A), and the binding energy was −7.23 kcal/mol. According to Figs. 4B and C, liquiritin could form strong hydrogen bond interactions with THR-30, ASN-85, HIS-261, MET-109 and THR-106 of the protein active site, and the average length of hydrogen bond distance was 2.36 Å. Meanwhile, the compound also had good hydrophobic interaction withPHE-257, THR-30, VAL-34, MET-109, THR-106, VAL-265, PHE-239, contributing to the stability of small molecules. Therefore, liquiritin could form a stable complex with MRGPRX2.

As suggested by the QRT-PCR validation of MRGPRX2-HEK293T and NC-HEK293T cell construction (Fig. 4D), the MRGPRX2 receptor expression by the MRGPRX2-HEK293T cells was successful. We observed no response of intracellular Ca^{2+} after C48/80 or liquiritin treatment in NC-HEK293T cells (Fig. 4E). While in MRGPRX2-HEK293T cells (Fig. 4F), compared with the blank control and C48/80 groups, liquiritin dose-dependently reduced the C48/80-elicited calcium influx. In conclusion, liquiritin's anti-pseudo-allergic action was considered to be associated with MRGPRX2.

3.5. *Liquiritin inhibited Ca^{2+}-Related PI3K/AKT and PLCγ signaling pathways*

The Ca^{2+} signaling pathway is critical to the degranulation of MCs. Our recent study suggested that in PARs, MrgprX2 regulated the degranulation of MCs via Ca^{2+}-associated PI3K/AKT and PLCγ signaling [14]. In this study, as Ca^{2+} influx was inhibited significantly by liquiritin, we investigated its effects on PI3K/AKT and PLCγ using Western blot analysis. According to Figs. 5A and B, liquiritin dose-dependently reduced the phosphorylation of PI3K, Akt and PLCγ in MPMCs. For further verification, the expression of related proteins was determined in the paw skin tissue of mice. The results also demonstrated that liquiritin dose-dependently decreased the phosphorylation of PI3K, Akt and PLCγ (Figs. 6A and B). Therefore, our results suggested that liquiritin inhibited pseudo-allergy via the PLCγ and PI3K/AKT pathways.

4. Discussion

PARs are a widespread consequence of functional food or drug intake, in which MCs are primary effectors implicated by discharging diverse inflammatory mediators and histamine, and such a mechanism is known as degranulation [15]. MRGPRX2, being a

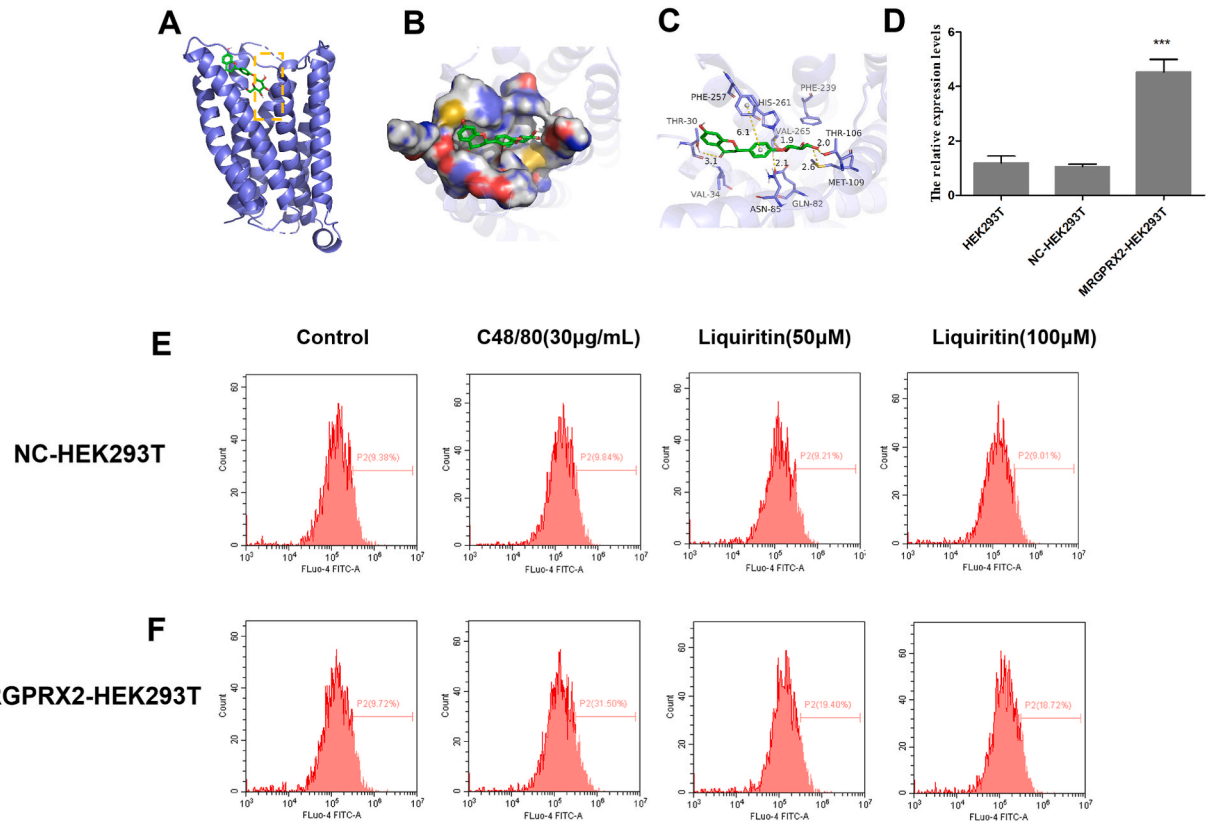

Fig. 4. Liquiritin has potential as a MRGPRX2 ligand. (A) 3D structural depiction of liquiritin–MRGPRX2 complex. (B) The electrostatic surface of liquiritin with MRGPRX2 protein. (C) The detail binding mode of liquiritin with MRGPRX2 protein. Yellow dash represented hydrogen bond distance. (D) QRT-PCR validation of successful MRGPRX2-HEK293T and NC-HEK293T cell construction. (E) Both C48/80 and liquiritin did not induce intracellular Ca^{2+}concentration in NC-HEK-293 cells. (F) Liquiritin dose dependently reduced the calcium influx elicited by C48/80 in MRGPRX2-HEK293T cells.

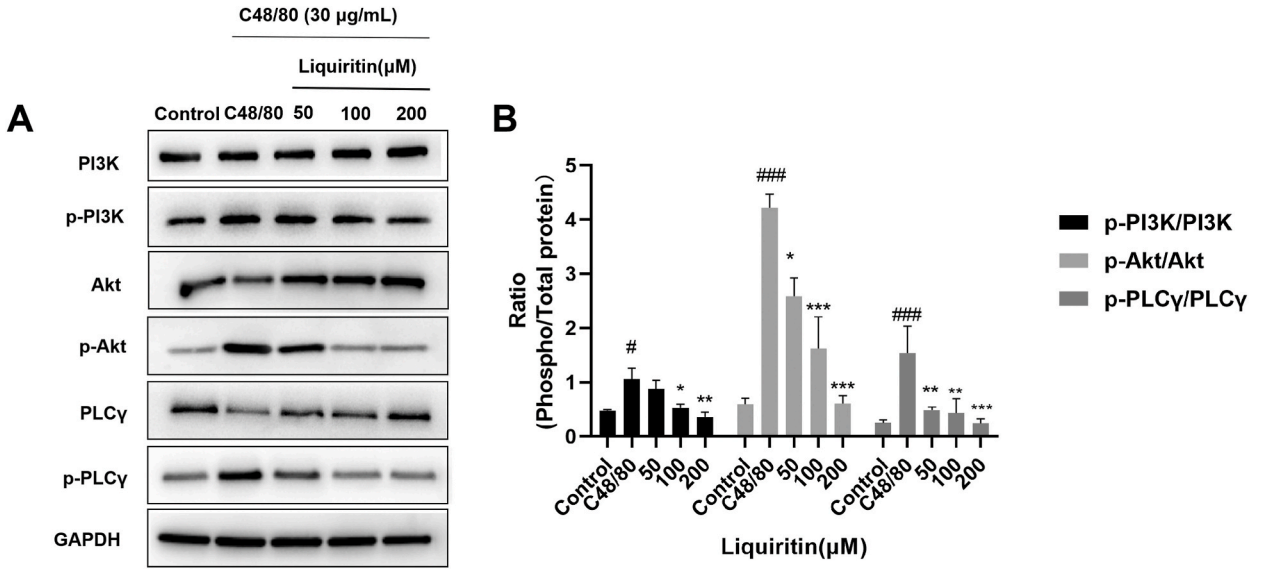

Fig. 5. Liquiritin reduced the phosphorylation of PI3K, Akt andPLCγ in a dose-dependent manner in MPMCs. (A) Western blot findings for the expression and phosphorylation levels of PI3K, Akt and PLCγ. (B) Densitometric findings concerning related protein expression in (A). Data expressed are means ± SEMs (n = 3). $^{###}p < 0.001$, C48/80 group vs. control group. $^{*}p < 0.05$, $^{**}p < 0.01$, $^{***}p < 0.001$, treatment groups vs. C48/80 group.

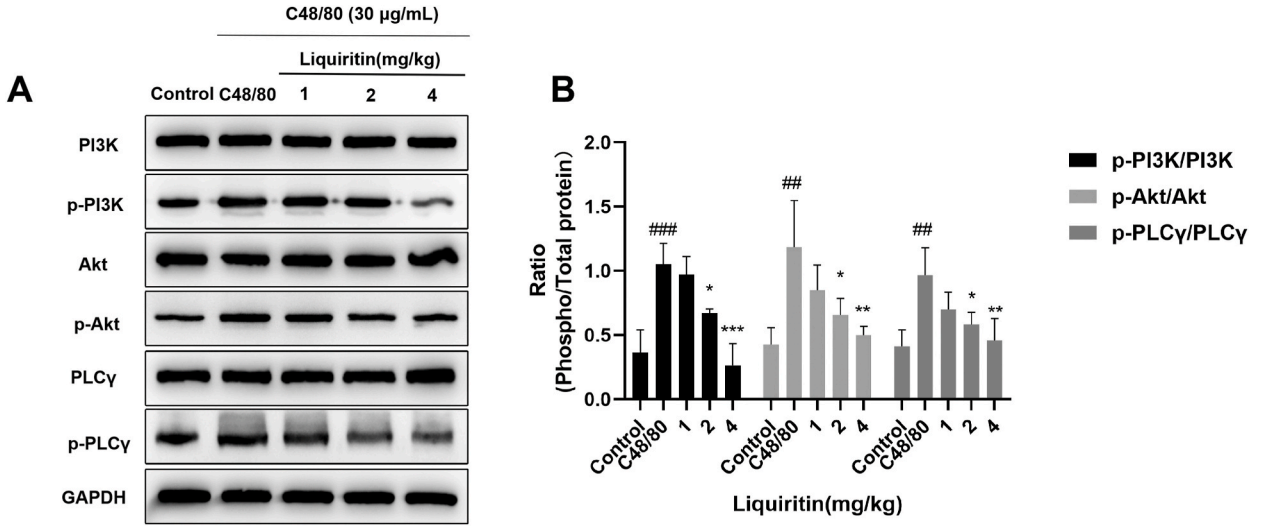

Fig. 6. Liquiritin reduced the phosphorylation of PI3K, Akt and PLCγ dose-dependently *in vivo*. (A) Western blot findings for the expression and phosphorylation levels of PI3K, Akt and PLCγ. (B) Densitometric findings concerning related protein expression in (A). Data expressed are means ± SEMs (n = 3). $^{##}p < 0.01$, $^{###}p < 0.001$, C48/80 group vs. control group. $^{*}p < 0.05$, $^{**}p < 0.01$, $^{***}p < 0.001$, treatment groups vs. C48/80 group.

specific receptor, either facilitates the MC-dependent host defense and immunomodulation, or acts as a pathogenetic factor for PARs [2]. Therefore, novel MRGPRX2 antagonists have attracted much more attention [16]. This study investigated the anti-pseudo-allergic effect and potential mechanisms of liquiritin as a potential treatment for PARs for the first time. The results demonstrated that apart from suppressing the degranulation and calcium influx elicited by C48/80 *in vitro*, liquiritin also suppressed the vascular leakage and edema in the hind paw, and led to declined levels of histamine and TNF-α *in vivo*. Besides, liquiritin was identified as a potential MRGPRX2 ligand, which regulated the calcium-related PI3K/AKT and PLCγ signaling pathways.

Clinically, anaphylaxis is usually treated by drug withdrawal or injection of glucocorticoids such as dexamethasone or antihistamines such as promethazine [17]. However, such drugs only work in the symptom control stage downstream of the allergic reaction mechanism, and allergic mediators still exist in the body. In addition, prolonged use of the foregoing drugs will produce varying side effects. There are still no specific and acknowledged drugs for the prevention and alleviation of PARs mediated by MRGPRX2, nor are

there any established uniform diagnostic criteria for the disease. Therefore, finding a safe and effective natural ingredient for PARs is still of great concern.

It has been reported that triterpenoid saponins in licorice, such as glycyrrhizic acid and glycyrrhetinic acid, play an anti-allergic role due to their mild glucocorticoid-like effects [18]. Liquiritin, as a flavonoid, was reported to inhibit MRGPRX2-mediated PARs in our study for the first time. Previously, we discovered the inhibitory action of licorice extract against C48/80-triggered degranulation of MCs, and licochalcone A was screened to be a potential MRGPRX2 ligand by RBL-2H3 cell extraction [19], which is also consistent with a similar study on licochalcone A's anti-pseudo-allergy function [20]. In addition, isoliquiritigenin was also reported to possess anti-pseudo-allergy potential [21]. Interestingly, liguiritin, licochalcone A and isoliquiritigeninare are all flavonoids, the physiological activity of which is closely related to their chemical structure. Such as the parent nucleus, substituent group, substitution mode and number of flavonoids. These findings indicated that flavonoids in licorice were promising candidates for the treatment of PARs. Because the structure of flavonoids has a strong regularity, further screening and structure-activity relationship analysis of flavonoids in licorice may help to find anti-pseudo-allergic components with better activity.

Owing to its ability to facilitate the degranulation of MCs, C48/80 is adopted widely in PAR research, which is a condensation product of N-methyl *p*-methoxyphenethylamine with formaldehyde [22]. Our previous study suggested the regulatory roles of PI3K/AKT axis and PLCγ in the C48/80-triggered degranulation response of MCs as downstream signals of MRGPRX2, which was achieved by affecting the intracellular concentration of Ca^{2+} [14]. The present work demonstrated that liquiritin suppressed PARs through downregulating the phosphorylation of PI3K/AKT and PLCγ, which supplied an option for the prevention and alleviation of pseudo-allergy.

In conclusion, we elucidated the anti-pseudo-allergic effect and mechanisms of liquiritin, which has tremendous potential as a cost-efficient anti-pseudo-allergic agent. Our findings would lay a basis for the novel drug development, and offer a new insight into the allergic disease prevention and management.

Author contribution statement

Lu Wang: Conceived and designed the experiments; Performed the experiments; Contributed reagents, materials, analysis tools or data; Wrote the paper.

Chuyue Huang: Performed the experiments; Wrote the paper.

Zhili Li: Performed the experiments.

Guizhou Hu: Analyzed and interpreted the data; Wrote the paper.

Jin Qi: Analyzed and interpreted the data.

Zhimin Fan: Conceived and designed the experiments; Contributed reagents, materials, analysis tools or data.

Funding statement

Dr. Lu Wang was supported by National Natural Scientific Foundation of China [81903788].

Data availability statement

Data included in article/supp. material/referenced in article.

Declaration of interest's statement

The authors declare that they have no known competing financial interests or personal relationships that could have appeared to influence the work reported in this paper.

Appendix A. Supplementary data

Supplementary data to this article can be found online at https://doi.org/10.1016/j.heliyon.2023.e13290.

References

[1] H. Subramanian, K. Gupta, H. Ali, Roles of Mas-related G protein-coupled receptor X2 on mast cellmediated host defense, pseudoallergic drug reactions, and chronic inflammatory diseases, J. Allergy Clin. Immunol. 138 (2016) 700–710.

[2] B.D. McNeil, P. Pundir, S. Meeker, L. Han, B.J. Undem, M. Kulka, X.D. Dong, Identification of a mast-cellspecific receptor crucial for pseudo-allergic drug reactions, Nature 519 (2015) 237–241.

[3] S.W. Han, L. Sun, F. He, H.L. Che, Anti-allergic activity of glycyrrhizic acid on IgE-mediated allergic reaction by regulation of allergy-related immune cells, Sci. Rep. 7 (2017), 7222.

[4] M. Cheng, J. Zhang, L. Yang, S. Shen, P. Li, S. Yao, H. Qu, J. Li, C. Yao, W. Wei, D.A. Guo, Recent advances in chemical analysis of licorice (Gan-Cao), Fitoterapia 149 (2021), 104803.

[5] M.Y. Jiang, S.J. Zhao, S.S. Yang, X. Lin, X.G. He, X.Y. Wei, Q. Song, R. Li, C.M. Fu, J.M. Zhang, Z. Zhang, An "essential herbal medicine"-licorice: a review of phytochemicals and its effects in combination preparations, J. Ethnopharmacol. 249 (2020), 112439.

[6] X.H. Yang, X.W. Dang, X. Zhang, S.R. Zhao, Liquiritin reduces lipopolysaccharide-aroused HaCaT cell inflammation damage via regulation of microRNA-31/MyD88, Int. Immunopharm. 101 (2021), 108283.
[7] H.D. Ni, M. Xu, K.Y. Xie, Y. Fei, H.S. Deng, Q.L. He, T.T. Wang, S.L. Liu, J.J. Zhu, L.S. Xu, M. Yao, Liquiritin alleviates pain through inhibiting CXCL1/CXCR2 signaling pathway in bone cancer pain rat, Front. Pharmacol. 11 (2020) 436.
[8] X. Li, X.M. Qin, J.S. Tian, X.X. Gao, X.K. Wu, G.H. Du, Y.Z. Zhou, Liquiritin protects PC12 cells from corticosterone-induced neurotoxicity via regulation of metabolic disorders, attenuation ERK1/2-NF-κB pathway, activation Nrf2-Keap1 pathway, and inhibition mitochondrial apoptosis pathway, Food Chem. Toxicol. 146 (2020), 111801.
[9] W. Zhang, T. Li, X.J. Zhang, Z.Y. Zhu, Hypoglycemic effect of glycyrrhizic acid, a natural non-carbohydrate sweetener, on streptozotocin-induced diabetic mice, Food Funct. 11 (2020) 4160–4170.
[10] V.T. Thu, N.T.H. Yen, N.T.H. Ly, Liquiritin from *radix glycyrrhizae* protects cardiac mitochondria from hypoxia/reoxygenation damage, J Anal Methods Chem 2021 (2021), 1857464.
[11] M. Babina, Z. Wang, K. Franke, S. Guhl, M. Artuc, T. Zuberbi, Yin-yang of IL-33 in human skin mast cells: reduced degranulation, but augmented histamine synthesis through p38 activation, J. Invest. Dermatol. 139 (2019) 1516–1525.
[12] K. Lansu, J. Karpiak, J. Liu, X.P. Huang, J.D. McCorvy, W.K. Kroeze, T. Che, H. Nagase, F.I. Carroll, J. Jin, B.K. Shoichet, B.L. Roth, In silico design of novel probes for the atypical opioid receptor MRGPRX2, Nat. Chem. Biol. 13 (2017) 529–536.
[13] J.L. Wang, Y.J. Zhang, J. Wang, R. Liu, G.P. Zhang, K. Dong, T. Zhang, Paeoniflorin inhibits MRGPRX2-mediated pseudo-allergic reaction via calcium signaling pathway, Phytother Res. 34 (2020) 401–408.
[14] F. Zhang, F. Hong, L. Wang, R.J. Fu, J. Qi, B.Y. Yu, MrgprX2 regulates mast cell degranulation through PI3K/AKT and PLCγ signaling in pseudo-allergic reactions, Int. Immunopharm. 102 (2022), 108389.
[15] H. Ogasawara, M. Furuno, K. Edamura, M. Noguchi, Novel MRGPRX2 antagonists inhibit IgE-independent activation of human umbilical cord blood-derived mast cells, J. Leukoc. Biol. 106 (2019) 1069–1077.
[16] W.J. Pichler, Immune pathomechanism and classification of drug hypersensitivity, Allergy 74 (2019) 1457–1471.
[17] J.M. Moodley, J.C. Gardner, D.J. Sheridan, Why remove injectable promethazine from the formulary? Nursing 50 (2020) 13.
[18] Y. Nishimoto, A. Hisatsune, H. Katsuki, T. Miyata, K. Yokomizo, Y. Isohama, Glycyrrhizin attenuates mucus production by inhibition of MUC5AC mRNA expression in vivo and in vitro, J. Pharmacol. Sci. 113 (2010) 76–83.
[19] L. Wang, G.Z. Hu, Y. Lu, S.J. Jiang, J. Qi, H. Su, Anti-pseudo-allergic components in licorice extract inhibit mast cell degranulation and calcium influx, Chin. J. Nat. Med. 20 (2022) 421–431.
[20] Z.L. Xue, Y.J. Zhang, Y.N. Zeng, S.L. Hu, H.Y. Bai, J. Wang, H.L. Jing, N. Wang, Licochalcone A inhibits MAS-related GPR family member X2-induced pseudo-allergic reaction by suppressing nuclear migration of nuclear factor-κB, Phytother Res. 35 (2021) 6270–6280.
[21] Y.J. Hou, D.L. Che, P.Y. Ma, T.T. Zhao, Y.N. Zeng, N. Wang, Anti-pseudo-allergy effect of isoliquiritigenin is MRGPRX2-dependent, Immunol. Lett. 198 (2018) 52–59.
[22] S.W. Kashem, H. Subramanian, S.J. Collington, P. Magotti, J.D. Lambris, H. Ali, G protein coupled receptor specificity for C3a and compound 48/80-induced degranulation in human mast cells: roles of Mas-related genes MrgX1 and MrgX2, Eur. J. Pharmacol. 68 (2011) 299–304.